Mechanism of large magnetoresistance in $Co_2MnSi/Ag/Co_2MnSi$ devices with current perpendicular to the plane

Y. Sakuraba,* K. Izumi, T. Iwase, S. Bosu, K. Saito, and K. Takanashi
Institute for Materials Research (IMR), Tohoku University, Katahira 2-1-1, Aoba-ku, Sendai 980-8577, Japan

Y. Miura, K. Futatsukawa, K. Abe, and M. Shirai
Research Institute of Electrical Communication (RIEC) and Center for Spintronics Integrated Systems (CSIS), Tohoku University, Katahira 2-1-1, Aoba-ku, Sendai 980-8577, Japan

(Received 5 July 2010; revised manuscript received 23 August 2010; published 28 September 2010)

Fully epitaxial current-perpendicular-to-plane giant magnetoresistance (MR) devices with half-metallic Co_2MnSi (CMS) electrodes and a Ag spacer were fabricated to investigate the relationship between the chemical ordering in CMS and its MR properties, including bulk and interface spin-asymmetry coefficients β and γ. CMS/Ag/CMS annealed at 550 °C shows the largest MR ratio: 36.4% and 67.2% at RT and 110 K, respectively. An analysis based on Valet-Fert's model reveals large spin asymmetry ($\gamma > 0.8$) at the CMS/Ag interface, which contributes predominantly to the large MR ratio observed. First-principles ballistic conductance calculations for (001)-CMS/Ag/CMS predict a high majority-spin electron conductance, which could be the origin of the large γ observed in this study.

DOI: 10.1103/PhysRevB.82.094444 PACS number(s): 75.76.+j, 85.75.−d

I. INTRODUCTION

A current-perpendicular-to-plane giant magnetoresistance (CPP-GMR) device, consisting of two ferromagnetic layers separated by a nonmagnetic spacer, is one of promising candidates for next generation magnetic read head of high-density hard disk drive (HDD), since it has small resistance area product (RA) suitable for high-speed reading.[1,2] However, the critical disadvantage of CPP-GMR devices is a small MR ratio, i.e., small signal/noise ratio, compared with that in magnetic tunnel junctions (MTJs). In addition, there is a limitation of total film thickness in MR devices for a magnetic read head to fit a narrow read gap length in high-density HDD. Therefore it is necessary to improve MR ratio in CPP-GMR devices by a dominant contribution of ferromagnetic layer/nonmagnetic layer interface scattering in order to apply to a magnetic read head.

Half-metallic ferromagnets (HMFs), which possess perfectly spin-polarized conduction electrons because of a semiconducting gap in either the up- or down-spin channel at the Fermi level, are attracting much interest in spintronics research because they are expected to enhance and elicit various spin-dependent phenomena and improve the performance of applications. Recently, several Co-based Heusler compounds, a class of HMFs, such as Co_2MnSi (CMS), Co_2MnGe, and $Co_2FeAl_{0.5}Si_{0.5}$, have been applied as ferromagnetic electrodes in MTJs (Refs. 3–10) and CPP-GMR devices[11–17] to enhance the MR properties. An extremely large MR ratio of 560% at 2 K has already been reported in MTJs with CMS electrodes and an amorphous Al-O tunneling barrier, indicating clearly the half metallicity of CMS at low temperature.[4] Larger MR ratios have been also achieved by combining a Heusler compound electrode with MgO or $(MgAl_2)O_x$ crystalline tunneling barrier.[5–10] Shan *et al.*[9] has recently reported relatively small temperature dependence of tunneling MR (TMR) ratio in $Co_2FeAl_{0.5}Si_{0.5}$-based MTJs with $(MgAl_2)O_x$ barrier and claimed the demonstration of half metallicity at room temperature (RT) according to the fitting of TMR vs T curve based on the magnon excitation model, i.e., they found large intrinsic spin polarization of $Co_2FeAl_{0.5}Si_{0.5}$ at RT when the depolarization effect due to the thermally excited magnon at the barrier interface was excluded. Even in that study, however, observed MR ratio was just 102% at RT which was much smaller than that observed in general CoFeB/MgO/CoFeB MTJs.[18] Thus, it was suggested that the spin flipping caused by thermally excited magnon is actually a critical obstacle to obtain a giant TMR ratio reflecting half metallicity at RT in MTJs. On the other hand, in contrast to the MTJs, recent studies on CPP-GMR using half-metallic Heusler compounds showed large MR ratio even at RT. A large MR ratio of 28.8% and a resistance change area product (ΔRA) of 8.9 $m\Omega\ \mu m^2$ at RT were achieved in an (001)-oriented fully epitaxial CMS/Ag/CMS CPP-GMR device, which was much higher than typical MR ratios (less than 3%) in CPP-GMR devices based on 3d-ferromagnetic materials (CoFe, etc.),[19] indicating high spin polarization in CMS even at RT. Mavropoulos *et al.*[20] predicted that the spin-flip processes, which attributes to the remarkable temperature dependence of the TMR via electronic states in the minority-spin gap near the electrode/barrier interfaces, does not play a crucial role in the present CPP-GMR devices, since spin accumulation at the electrode/spacer interface could be less than that at the electrode/barrier interfaces in the MTJs. Thus, CPP-GMR structure is promising to extract half metallicity at RT.

Heusler compounds, which have a general formula X_2YZ and crystallize in the $L2_1$ structure, also grow in the chemically disordered $B2$ (or $A2$) structure, in which Y and Z (or X, Y, and Z) are randomly substituted. Some theoretical studies of the electronic structure of CMS and Co_2CrAl have reported that the half-metallic electronic structure is sensitive to chemical disordering;[21,22] half metallicity was predicted to be preserved in $B2$ disordering but perfectly destroyed in $A2$ disordering, especially by the Co antisite. Recently a large

depolarization effect of Co antisite to the TMR effect has been confirmed in the CMS-based MTJs by changing the Co composition in CMS systematically.[23] In previous studies of a half-metallic Heusler-compound-based CPP-GMR, however, a systematic analysis of the crystal structure, chemical ordering, and magnetic properties of CMS against the MR properties was missing. Moreover, bulk and interface spin-scattering contributions to the MR effect have not been analyzed quantitatively in CMS/Ag/CMS CPP-GMR devices. Therefore, the mechanism for the large MR effect observed in CMS/Ag/CMS and the relationship between MR and chemical ordering is still unclear. In the present study, bulk and interface spin-asymmetry coefficients β and γ, respectively, are studied quantitatively in CMS/Ag/CMS on the basis of Valet and Fert's model.[24] The relationships between the MR properties (i.e., MR ratio, ΔRA, β, and γ) and the structural and magnetic properties are systematically investigated. Finally, the origin of the large MR ratio in CMS/Ag/CMS is discussed by comparing the experimental results with first-principles ballistic conductance calculations.

II. SAMPLE PREPARATION AND EXPERIMENTAL METHOD

Fully epitaxial CMS/Ag/CMS films were prepared by an ultrahigh-vacuum-compatible magnetron sputtering system ($P_{base} < 1 \times 10^{-7}$ Pa). First, Cr (20 nm)/Ag (40 nm) buffer layers were deposited on a MgO (001) single-crystal substrate at RT to improve the surface flatness. A lower CMS layer was also grown at RT using a $Co_{43.7}Mn_{28.0}Si_{28.4}$ alloy target followed by *in situ* annealing to promote chemical ordering. Electron probe microanalysis showed a nearly stoichiometric Co-Mn-Si composition in the CMS layer (Co:Mn:Si=50.4:25.0:24.6). For systematic investigation, the annealing temperature (T_{ann}) and CMS thickness (t_{CMS}) were varied from 350 to 650 °C and 3 nm to 11 nm, respectively. After the sample was cooled to RT, a 5-nm-thick Ag spacer and an upper CMS layer were deposited. The thickness and annealing temperature of the upper CMS in each sample were the same as those of the lower CMS. Finally, the film was capped by Ag(2 nm)/Au(5 nm) protective layers. The film was patterned into pillars for CPP-type four-terminal device structures using electron-beam lithography and Ar-ion milling. The designed size of the pillars changed from 100×200 to 300×600 nm^2 on one substrate.

The MR characteristics were measured by the dc four-terminal method by applying a magnetic field to the CMS⟨110⟩ easy magnetization axis direction. CMS single-layer films (i.e., MgO-subs./Cr/Ag/CMS) 30 nm thick with different T_{ann} were also prepared to check their crystal structure, chemical ordering, and magnetic properties using x-ray diffraction (XRD) with Cu $K\alpha$ radiation and a vibrating sample magnetometer. The ratio of $L2_1$- and $B2$-superlattice peaks intensity to fundamental peak intensity, $\alpha_{obs}^{L2_1}$ and α_{obs}^{B2}, respectively, was evaluated by using the following formulas:

$$\alpha_{obs}^{L2_1} = \frac{I_{obs}(111)/I_{obs}(220)}{I_{cal}(111)/I_{cal}(220)}, \quad \alpha_{obs}^{B2} = \frac{I_{obs}(200)/I_{obs}(400)}{I_{cal}(200)/I_{cal}(400)}, \tag{1}$$

where $I_{obs}(111)$ and $I_{obs}(200)$ denote the integrated intensity of superlattice peaks for the $L2_1$ and $B2$ ordering, respectively, and $I_{obs}(220)$ and $I_{obs}(400)$ denote that of the corresponding fundamental peaks. Here, $I_{cal}(hkl)$ represents the (hkl) peak intensity calculated by assuming a perfect $L2_1$ ordering structure.

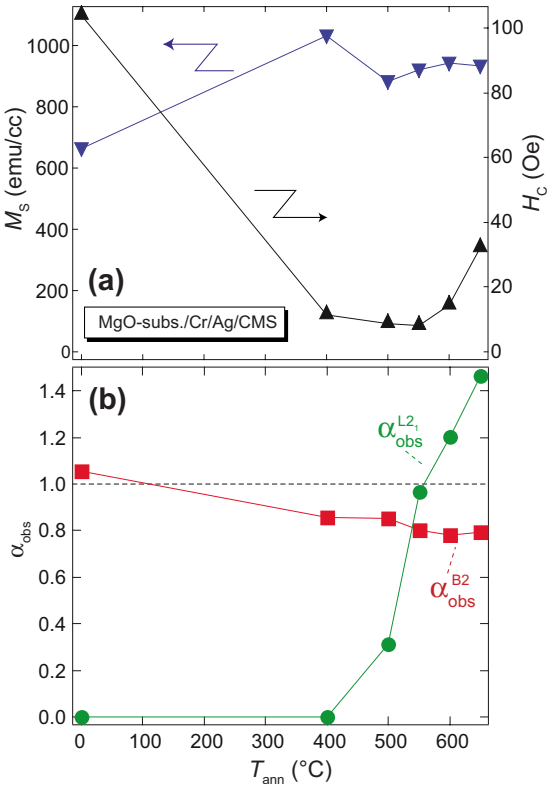

FIG. 1. (Color online) Annealing temperature dependence of (a) M_S, H_C and (b) α_{obs} in CMS single-layer films.

III. EXPERIMENTAL RESULT

Figure 1 shows the T_{ann} dependence of the saturation magnetization M_S, coercive field H_C, and α_{obs} in CMS single-layer films. Although M_S was close to a bulk value (~1050 emu/cc) over the entire T_{ann} range, H_C increased slightly at temperatures above T_{ann}=600 °C, indicating slight interdiffusion between the CMS and Ag layers. The XRD profiles for the CMS films confirmed a (001)-oriented epitaxial growth for the entire T_{ann} range. The estimated α_{obs}^{B2} was almost equal to unity even before annealing and gradually decreased slightly with increasing T_{ann}. In contrast, the $\alpha_{obs}^{L2_1}$ was 0 in the as-deposited state and improved after annealing at temperatures above 500 °C. Interestingly, with increasing annealing temperature, $\alpha_{obs}^{L2_1}$ became larger than α_{obs}^{B2} at 550 °C and finally exceeded unity above 600 °C, and also α_{obs}^{B2} gradually reduced from unity. This behavior cannot be explained by considering only $B2$- and $A2$-type disorderings from $L2_1$ structure in CMS. In order to explain it, it is necessary to consider $D0_3$-type disordering in CMS, i.e., preferential substitutions between Co and Mn atoms in the $L2_1$ structure such as $(Co_{1-x/2}Mn_{x/2})_2(Mn_{1-x}Co_x)Si$, Fig. 2 shows the simulated α_{obs} against the amount of $D0_3$ disordering x. When $D0_3$ disordering occurs in CMS, $L2_1$- and

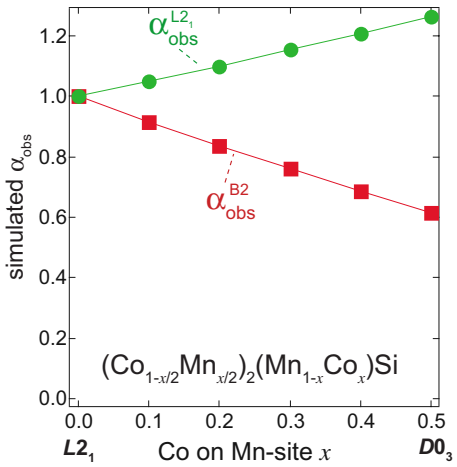

FIG. 2. (Color online) Simulated α_{obs} against the amount of Co-Mn disordering in CMS.

$B2$-superlattice peaks increase and decrease, respectively. Thus $\alpha_{obs}^{L2_1}$ increases and α_{obs}^{B2} reduces from unity with $D0_3$ disordering x. Therefore, we conclude that the $L2_1$ ordering in our epitaxial CMS film was promoted by annealing; at the same time, however, the $D0_3$ disordering increased slightly in the CMS with annealing. A certain amount of $D0_3$ disordering between Co and Mn with no disordering of Si has also been found even in a CMS single-crystal specimen using neutron diffraction.[25]

The annealing temperature dependence of the maximum MR ratio in CMS/Ag/CMS is shown in Fig. 3. The result for CMS/Cr/CMS is also plotted for comparison. In CMS/Cr/CMS, although the MR ratio was improved by annealing at T_{ann}=350 °C as reported in Ref. 13, the MR effect disappeared after annealing at 500 °C because of large interdiffusion between CMS and Cr. In CMS/Ag/CMS, however, the MR ratio continued to increase up to 550 °C, which is mainly because of the small solubility of Ag into CMS compared with that of Cr. Finally, the largest MR ratio of 36.4% at RT and 67.2% at 110 K were observed for CMS/Ag/CMS prepared at T_{ann}=550 °C. The ΔRA in corresponding sample was 11.5 $m\Omega\cdot\mu m^2$ at RT. Ag/CMS does not increase monotonically with decreasing temperature and takes a maximum around 100 K. The origin of this behavior against temperature will be discussed elsewhere.

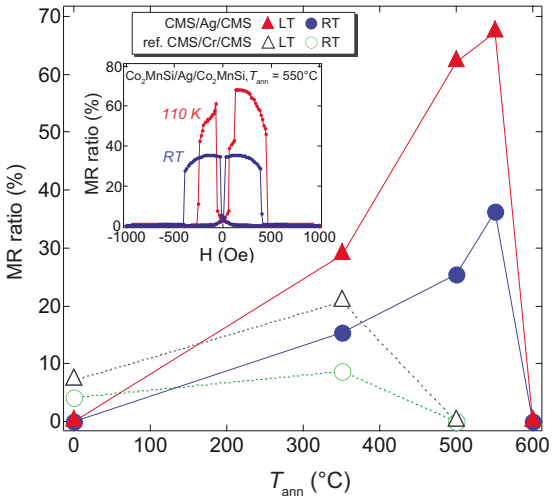

FIG. 3. (Color online) Annealing temperature dependence of maximum MR ratio for CMS/Ag/CMS and CMS/Cr/CMS. Inset shows MR curves showing maximum MR ratio for CMS/Ag/CMS annealed at 550 °C.

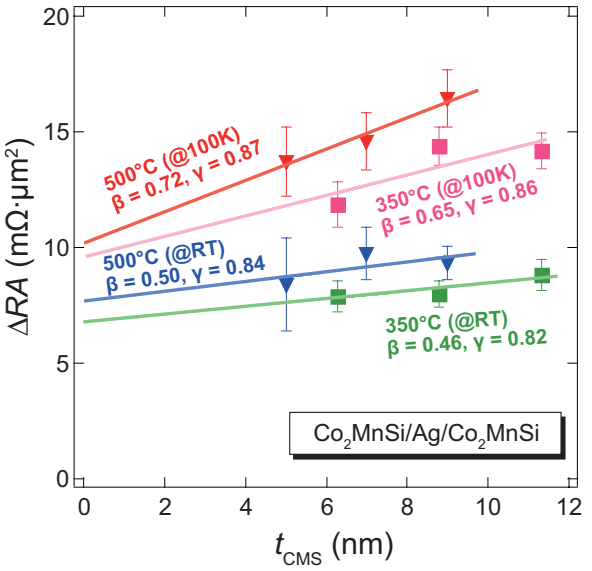

FIG. 4. (Color online) CMS thickness dependence of ΔRA in CMS/Ag/CMS annealed at 350 and 500 °C. Solid curves are fitting results using Eq. (2).

The bulk and interface spin-asymmetry coefficients of electron scattering (β and γ) in CMS/Ag/CMS prepared at T_{ann}=350 and 500 °C were quantitatively analyzed. Figure 4 shows the CMS thickness (t_{CMS}) dependence of ΔRA measured at RT and 100 K. ΔRA monotonically increased with t_{CMS} up to 11 nm, indicating the spin-diffusion length of our CMS electrode is longer than 11 nm and that observed in the $Co_2FeAl_{0.5}Si_{0.5}$ electrode.[12] Thus, here the data were fitted by the following equation based on Valet-Fert's model without the spin-diffusion length of CMS:

$$\Delta RA = \frac{(2\beta\rho^*_{CMS}t_{CMS} + 2\gamma R^*_{CMS/Ag}A)^2}{2\rho^*_{CMS}t_{CMS} + 2R^*_{CMS/Ag}A + \rho_{Ag}t_{Ag}}, \qquad (2)$$

where ρ^*_{CMS} and $R^*_{CMS/Ag}$ are the bulk resistivity of CMS (ρ_{CMS}) and interfacial resistance between CMS and Ag ($R_{CMS/Ag}$) considering spin asymmetries, respectively, i.e., $\rho^*_{CMS}=\rho_{CMS}/(1-\beta^2)$ and $R^*_{CMS/Ag}=R_{CMS/Ag}/(1-\gamma^2)$. Here, A is the perpendicular cross-sectional area of the pillars; ρ_{Ag} and t_{Ag} are the resistivity and thickness of the Ag layer, respectively. We evaluated ρ_{CMS} to be 40.2 $\mu\Omega$ cm at RT and 32.6 $\mu\Omega$ cm at 100 K by measuring the resistances of the CMS films. We obtained a value of 1.62 mΩ μm^2 for $R_{CMS/Ag}$ from first-principles calculations, and this value was used for fitting the experimental data at both RT and 100 K. This is justified because previous studies[26,27] found good agreement between experimental and calculated interface resistances, especially in epitaxially grown films, as well as a very small temperature dependence of the interface resistance. Curves fitted to the experimental data for the t_{CMS}

dependence of ΔRA are shown in Fig. 4 together with the values of β and γ thus obtained. Large spin asymmetry ($\gamma > 0.8$) at the CMS/Ag interface, obtained both at RT and 100 K, contributes predominantly to the large MR ratio observed in CMS/Ag/CMS. On the other hand, the fitting result for CMS/Cr/CMS (not shown here) confirms a small spin asymmetry ($\gamma < 0.4$) at the CMS/Cr interface, which is consistent with the small MR ratio observed in CMS/Cr/CMS compared with that in CMS/Ag/CMS even at the same T_{ann} in Fig. 3. Large interface scattering was also semiquantitatively suggested at the $Co_2Fe(Al_{0.5}Si_{0.5})/Ag$ interface in Ref. 12. Figures 3 and 4 clearly show that the enhancement of the MR ratio with increasing T_{ann} from 350 to 500 °C is due mainly to the increase in β rather than that in γ. We had inferred that promoting $L2_1$ ordering by annealing would improve the MR ratio much more than was observed. In contrast, however, the annealing also caused $D0_3$ disordering, which suppressed the MR ratio since Co antisites degraded the half metallicity of CMS, as predicted in Ref. 21. Therefore, suppressing the $D0_3$ disordering in the CMS layers could be a way to further enhance the MR ratio.

IV. DISCUSSION

Now, we discuss the origin of the difference in γ between CMS/Ag/CMS and CMS/Cr/CMS on the basis of first-principles ballistic conductance calculations using the quantum code ESPRESSO.[28] CMS/Ag/CMS and CMS/Cr/CMS trilayers were constructed in a tetragonal supercell containing 14 atomic layers of CMS and seven atomic layers of Ag or antiferromagnetic (AFM) Cr with MnSi termination. Other parameters of the first-principles calculations are the same as those in Ref. 29. Note that the conducting electrons are scattered only by the potential energy near the interface in the present ballistic transport formalism. Figures 5(a) and 5(b) show the in-plane wave-vector ($\boldsymbol{k}_\parallel$) dependence of the majority-spin conductance in the parallel magnetization configuration of CMS/Ag/CMS and CMS/Cr/CMS. The conducting channels of CMS/Cr/CMS are clearly restricted to a small region around $\boldsymbol{k}_\parallel=(0,0)$. On the other hand, highly conducting channels spread over almost the entire region in the $\boldsymbol{k}_\parallel$ plane for CMS/Ag/CMS. The highly conducting region in the $\boldsymbol{k}_\parallel$ plane can be understood qualitatively by considering the matching of the Fermi surface over the $\boldsymbol{k}_\parallel$ plane between CMS and Ag. Figures 5(c)–5(e) show the Fermi surfaces in the Brillouin zones of $L2_1$-CMS, fcc-Ag, and AFM bcc-Cr with a tetragonal unit cell. A large overlapping area of the Fermi surface appears on the $\boldsymbol{k}_\parallel$ plane between CMS and Ag, resulting in a small resistance area product ($2R_{CMS/Ag}A=3.21$ mΩ μm^2) of CMS/Ag/CMS, while the mismatching of the Fermi surface between CMS and Cr on the $\boldsymbol{k}_\parallel$ plane causes a large resistance area product ($2R_{CMS/Cr}A=16.1$ mΩ μm^2) of CMS/Cr/CMS. Although no conductance (infinite resistance) is expected in the minority-spin channel in ideal half metals, a finite resistance area product could appear in the minority-spin channel in real half metals for reasons such as atomic disorder, thermal fluctuation of magnetic moments, spin-orbit coupling, and so on. The minority-spin resistance area product reduces both β and

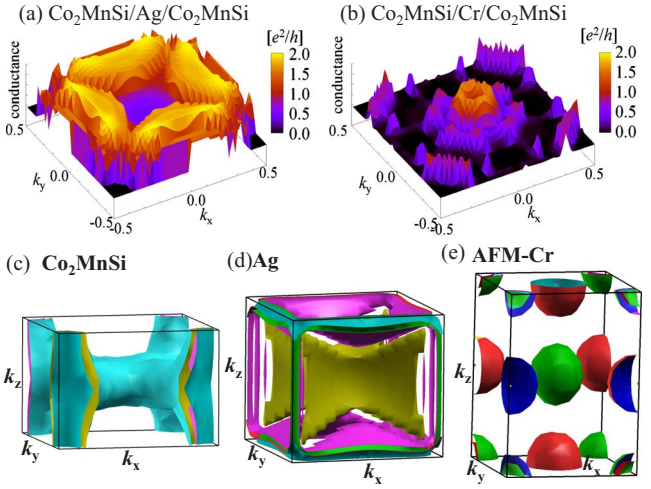

FIG. 5. (Color online) Majority-spin conductance in the parallel magnetization configuration calculated for (a) (001)-CMS/Ag/CMS and (b) (001)-CMS/Cr/CMS as a function of in-plane wave vector $\boldsymbol{k}_\parallel=(k_x,k_y)$. Fermi surfaces in the Brillouin zones corresponding to the tetragonal unit cell of (c) $L2_1$-CMS, (d) fcc-Ag, and (e) AFM bcc-Cr plotted by XCRYSDEN (Ref. 30).

γ. Thus, we can expect a larger value of γ for CMS/Ag/CMS than for CMS/Cr/CMS since the majority-spin resistance area product of CMS/Ag/CMS is much smaller than that of CMS/Cr/CMS. Experimentally, CMS/Ag/CMS and CMS/Cr/CMS with the same T_{ann}(=350 °C) and exactly the same stacking structure except for the spacer layer showed RA values of 51.4 mΩ μm^2 and 66.9 mΩ μm^2, respectively.[14] Here, the difference in RA (~15.5 mΩ μm^2) is caused mainly by the difference in interface resistances, i.e., $R_{CMS/Ag}A$ and $R_{CMS/Cr}A$ because the contribution of bulk resistance in the Ag and Cr spacers is negligibly small. Although the experimental RA is much higher than the calculated $2R_{CMS/NM}A$ (NM=Ag or Cr) because it includes all the resistances in the CPP pillars, the difference in RA, i.e., $2(R_{CMS/Cr}-R_{CMS/Ag})A$, is almost comparable to the calculated one (~12.9 mΩ μm^2). This quantitative agreement is evidence of a small interface resistance and large γ between CMS and Ag because of good Fermi-surface matching, as predicted by our calculations. Note that, large interface spin-asymmetry γ is an important characteristic for developing a magnetic read head based on CPP-GMR as mentioned in Sec. I.

V. SUMMARY

In conclusion, we fabricated (001)-oriented fully epitaxial CMS/Ag/CMS CPP-GMR devices with different CMS thicknesses and annealing temperatures to investigate the relationship between the magnetic properties, chemical ordering, and MR properties of CMS, including the bulk and interface spin-asymmetry coefficients β and γ. The analysis of XRD measurements reveals that annealing at temperatures above 500 °C enhanced the $L2_1$ ordering but also slightly increased the $D0_3$ disordering. CMS/Ag/CMS annealed at 550 °C showed the largest MR ratio: 36.4% and 67.2% at RT and

110 K, respectively. Analysis based on Valet-Fert's model suggests large spin asymmetry ($\gamma > 0.8$) at the CMS/Ag interface, which contributes predominantly to the large MR ratio observed. First-principles calculations of the ballistic conductance in the (001)-CMS/Ag/CMS structure predicted high majority-spin conductance because of the good Fermi-surface matching between CMS and Ag, which agreed quantitatively with the experimental *RA* and explained the large γ observed in the CMS/Ag/CMS well.

ACKNOWLEDGMENTS

The authors are deeply grateful to Y. Ando and T. Shima for giving us machine time for XRD and PPMS, respectively. This work was supported by Grants-in-Aid for Scientific Research in Priority Area "Creation and control of spin current" (Grants No. 19048002 and No. 19048004) from MEXT, and by the Japan Science and Technology (JST) agency through its Strategic International Cooperative Program under the title "Advanced spintronic materials and transport phenomena (ASPIMATT)." This work is part of a cooperative program of the ARCMG-IMR, Tohoku University.

*y.sakuraba@imr.tohoku.ac.jp

[1] M. Takagishi, K. Yamada, H. Iwasaki, H. N. Fuke, and S. Hashimoto, IEEE Trans. Magn. **46**, 2086 (2010).
[2] K. Nagasaka, A. Jogo, T. Ibusuki, H. Oshima, Y. Shimizu, and T. Uzumaki, Fujitsu Sci. Tech. J. **42**, 149 (2006).
[3] Y. Sakuraba, J. Nakata, M. Oogane, H. Kubota, Y. Ando, A. Sakuma, and T. Miyazaki, Jpn. J. Appl. Phys., Part 2 **44**, L1100 (2005).
[4] Y. Sakuraba, M. Hattori, M. Oogane, H. Kubota, Y. Ando, H. Kato, A. Sakuma, and T. Miyazaki, Appl. Phys. Lett. **88**, 192508 (2006).
[5] S. Tsunegi, Y. Sakuraba, M. Oogane, K. Takanashi, and Y. Ando, Appl. Phys. Lett. **93**, 112506 (2008).
[6] T. Ishikawa, T. Marukame, H. Kijima, K.-I. Matsuda, T. Uemura, M. Arita, and M. Yamamoto, Appl. Phys. Lett. **89**, 192505 (2006).
[7] T. Taira, T. Ishikawa, N. Itabashi, K.-I. Matsuda, T. Uemura, and M. Yamamoto, J. Phys. D: Appl. Phys. **42**, 084015 (2009).
[8] N. Tezuka, N. Ikeda, F. Mitsuhashi, and S. Sugimoto, Appl. Phys. Lett. **94**, 162504 (2009).
[9] R. Shan, H. Sukegawa, W. H. Wang, M. Kodzuka, T. Furubayashi, T. Ohkubo, S. Mitani, K. Inomata, and K. Hono, Phys. Rev. Lett. **102**, 246601 (2009).
[10] W. Wang, E. Liu, M. Kodzuka, H. Sukegawa, M. Wojcik, E. Jedryka, G. H. Wu, K. Inomata, S. Mitani, and K. Hono, Phys. Rev. B **81**, 140402(R) (2010).
[11] T. Furubayashi, K. Kodama, H. Sukegawa, Y. K. Takahashi, K. Inomata, and K. Hono, Appl. Phys. Lett. **93**, 122507 (2008).
[12] T. M. Nakatani, T. Furubayashi, S. Kasai, H. Sukegawa, Y. K. Takahashi, S. Mitani, K. Kodama, and K. Hono, Appl. Phys. Lett. **96**, 212501 (2010).
[13] Y. Sakuraba, T. Iwase, K. Saito, S. Mitani, and K. Takanashi, Appl. Phys. Lett. **94**, 012511 (2009).
[14] T. Iwase, Y. Sakuraba, S. Bosu, K. Saito, S. Mitani, and K. Takanashi, Appl. Phys. Express **2**, 063003 (2009).
[15] K. Yakushiji, K. Saito, S. Mitani, K. Takanashi, Y. K. Takahashi, and K. Hono, Appl. Phys. Lett. **88**, 222504 (2006).
[16] K. Nikolaev, P. Kolbo, T. Pokhil, X. Peng, Y. Chen, T. Ambrose, and O. Mryasov, Appl. Phys. Lett. **94**, 222501 (2009).
[17] T. Mizuno, Y. Tsuchiya, T. Machita, S. Hara, D. Miyauchi, K. Shimaawa, T. Chou, K. Noguchi, and K. Tagami, IEEE Trans. Magn. **44**, 3584 (2008).
[18] S. Ikeda, J. Hayakawa, Y. Ashizawa, Y. M. Lee, K. Miura, H. Hasegawa, M. Tsunoda, F. Matsukura, and H. Ohno, Appl. Phys. Lett. **93**, 082508 (2008).
[19] H. Yuasa, M. Yoshikawa, Y. Kamiguchi, K. Koi, H. Iwasaki, M. Yakagishi, and M. Sahashi, J. Appl. Phys. **92**, 2646 (2002).
[20] P. Mavropoulos, M. Ležaić, and S. Blügel, Phys. Rev. B **72**, 174428 (2005).
[21] S. Picozzi, A. Continenza, and A. J. Freeman, Phys. Rev. B **66**, 094421 (2002).
[22] Y. Miura, K. Nagao, and M. Shirai, Phys. Rev. B **69**, 144413 (2004).
[23] Y. Sakuraba, N. Hirose, M. Oogane, T. Nakamura, Y. Ando, and K. Takanashi, Appl. Phys. Lett. **96**, 092511 (2010).
[24] T. Valet and A. Fert, Phys. Rev. B **48**, 7099 (1993).
[25] M. P. Raphael, B. Ravel, Q. Huang, M. A. Willard, S. F. Cheng, B. N. Das, R. M. Stroud, K. M. Bussmann, J. H. Claassen, and V. G. Harris, Phys. Rev. B **66**, 104429 (2002).
[26] W. P. Pratt, Jr. and J. Bass, Appl. Surf. Sci. **256**, 399 (2009).
[27] W. Oepts, M. A. M. Gijs, A. Reinders, R. M. Jungblut, R. M. J. van Gansewinkel, and W. J. M. de Jonge, Phys. Rev. B **53**, 14024 (1996).
[28] S. Baroni, A. Dal Corso, S. de Gironcoli, and P. Giannozzi, http://www.pwscf.org
[29] Y. Miura, H. Uchida, Y. Oba, K. Abe, and M. Shirai, Phys. Rev. B **78**, 064416 (2008).
[30] A. Kokalj, Comput. Mater. Sci. **28**, 155 (2003).